Experimental and Numerical aspects of B416 Cu-Be alloy friction stir process

N. Lebaal[a], D. Chamoret[a], C. Langlade[a], A. Roman[a], D. Schlegel[b], E. Gete[a] and M. Folea[c]

a. ICB UMR 6303, CNRS, Univ. Bourgogne Franche-Comté, UTBM, 90010 Belfort Cedex, France
b. ESTA, 90000 Belfort Cedex, France
c. Univ. Transilvania de Brasov, ITMI, 500036, Brasov, Romania

Résumé :

Le procédé de malaxage est un nouveau procédé de durcissement superficiel des métaux, procédé simple, sans impact sur l'environnement et adaptable sur machine-outil conventionnelles ou à commande numérique pour en assurer une diffusion plus large. Une analyse expérimentale couplée à une étude numérique thermique de ce procédé sur des échantillons d'un alliage de cuivre au béryllium (B194) est proposée dans ce papier.

Abstract :

The Friction Stir Processing is an innovative surface engineering method, considered as a green processing technique. A good understanding of the process can be reached by the combined efforts of experimental examination and numerical modelling. In this study numerical and experimental investigations of Friction Stir Process (FSP) have been carried out on samples of B194 ASTM copper-beryllium alloy.

Friction Stir Processing, Non-linear thermal model , B194 ASTM copper-beryllium alloy

1 Introduction

One of the major advantages of Friction Stir Processing (FSP) as compared with other hardening superficial methods, lies in the fact that FSP is a simple and green technic that can be applied in situ on different components surfaces and which produces a local fine recrystallized layer enhancing mechanical properties, especially hardness. Moreover, based on the thermo-mechanical mixing of the surface of traded components without adding a supplementary material like in the case of coating, no weakness interface is created. Its principle based on friction stir welding (FSW) [9] is a simple thermo-mechanical process which employs arotating tool that moves along a workpiece surface under a normal load that produces strain and heat [4]. Thus, the friction between the tool and the work piece creates microstructure modifications by homogenization and refinement. The heat generation mechanism is influenced by the process parameters like normal load, rotational speed, transverse speed and geometric data concerning tool and work piece. Friction Stir Processing have been applied on different materials like aluminium,

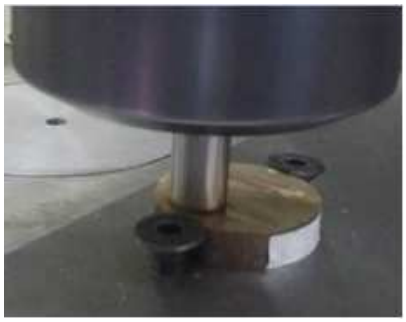

(a) Experimental device

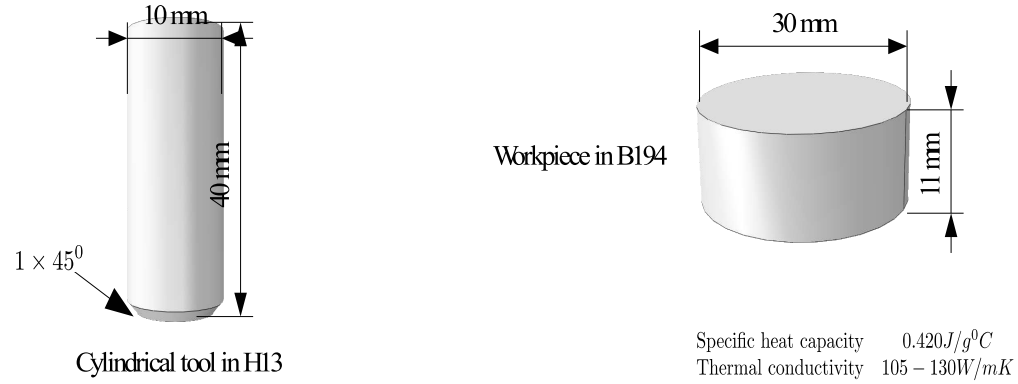

(b) FSP Data

FIGURE 1 – Friction Stir Process

titanium, steels [7, 9, 11, 6, 4]. This technique can also be applied to copper and copper alloys. Recently, Langlade et al. [6] in a study concerning FSP on B-416 copper beryllium alloy, concluded that this technique appears to be an appropriate superficial treatment method to improve local mechanical properties of this material, producing high hardness (approximately 260% higher that the initial value of the base material) and different thickness layers relative to process parameters. In addition, due to its importance for industrial applications, especially good oxidation and corrosion resistance as well as high electrical and thermal properties, $B194$ is a good candidate when hardening is needed only at the surface. Thus, the aim of this second study on $B-416$ is to characterize furthermore the FSP behavior of this material with regard to the phenomena of strain and heat generation by numerical simulation to elucidate the link between the FSP parameters and the prediction of the thickness of modified layers. Finally, the results of the numerical simulation will be compared to the experimental data.

2 Experimental Device

The main characteristics and forms of samples and tool used in this study are presented in Table 1 and Figure 1. The samples were processed by FSP using a 4-axis numerically controlled milling center (Gambin 50C) instrumented in force measuring, with a cylindrical tool in $H13$ of $10mm$ diameter, without pin.

In order to establish the functional relationship between friction stir process parameters (normal force, rotation speed and traverse speed) and the evolution of temperatures several cases have been studied. More specifically, in this paper, the influence of the normal force were investigated (Table 2). The pa-

Material	Be	Co+Ni	Co+Ni+Fe	Cu
	(wt%)	(wt%)	(wt%)	(wt%)
ASTM B194	1.8-2	0.2 min	0.60 max	Balance

TABLE 1 – Composition of B194

Trial	Traversal Speed $u\ (mm/min)$	Rotation speed r (rpm)	Normal Force $F_n(N)$	Measured Temperature $T\ (^0C)$
1	40	1000	1100	166
2	40	1000	1350	190

TABLE 2 – Combinations of FSP parameters

rameters have been retained taking into account the results obtained in previous works of Langlade et al. [6]. The temperature measurements during FSP have been made by infra-red technique with a Rayan CA1884 camera 2. For microstructure observations the specimens where cut perpendicularly to the processing trace by water jet and prepared by standard metallographic procedures. The samples was observed by optical (OM) and scanning electron microscopy (SEM).

3 Thermal Model of FSP

A physical understanding of the good process can be reached by the combined efforts of experimental examination and numerical modelling. To this end, A 3D non-linear thermal model was developed to simulate the thermal history. The simulated temperature distributions were compared with experimental values.

Thermal aspects appear highly important in the understanding of the FSP. From a physical point of view, the real process is thermomechanical because the thermal and mechanical aspects are coupled. From a numerical point of view, a purely thermal model can lead, like a modelling first step, to a good understanding of the FSP process. Moreover, these models are faster than thermomechanical ones and can be used as a first part of an uncoupled residual stress model or in optimisation process of FSP/FSW [8].

Several thermal models of FSP/FSW were developed describing the main heat source as friction between tool and workpiece and plastic deformation around the tool [1, 3, 5, 8, 10]. During the FSP, the tool moves along the workpiece surface. To model such motion, the moving heat source, is fairly complex. To facilitate the modelling, a different approach is used in this work : a moving coordinate system is fixed at the tool axis as in reference [12]. After making the coordinate transformation, the heat transfer problem becomes a convection-conduction problem that is straightforward to model. The model presented in this paper includes some simplifications and some important hypotheses.

— The heat generated at the tool shoulder/workpiece interface is frictional heat.
— No heat flows into the workpiece if the local temperature reaches the material melting temperature.

The following heat transfer model is used to evaluate the temperature fields produced in the workpiece during FSP. In the heat transfer analysis, the transient temperature (T) which is a function of time t and the spatial coordinates (x, y, z), is estimated by the three dimensional nonlinear heat transfer equation based on Fourier's law of heat conduction/convection :

$$\rho C_p \frac{\partial T}{\partial t} = \underbrace{k \triangle T}_{Conduction} - \underbrace{\rho C_p \, u \cdot \nabla T}_{Convection} + Q_{pin} \quad (1)$$

where ρ is the density, C_p the specific heat capacity, T the temperature, k the thermal conductivity, $q = -k\nabla T$ the heat flux and Q_{pin} is the heat generated by friction at the tool.

Equation (1) includes a convective term in addition to the conductive term. This is a consequence attachment of the coordinate system origin to the center tool axis. This is an original point compared to others thermal model of FSP where the convection is not considered [1].

In this study, only heat generation due to the friction between tool and the workpiece was considered. and the local heat flux generation (caused by the friction) per unit area (W/m^2) at the distance R from the center axis of the tool can be calculated by the following expression [2] :

$$Q_{pin}(R,T) = \begin{cases} \mu \frac{F_n}{A} \, R \, \omega & if \quad T < T_{melt} \\ 0 & Otherwise \end{cases} \quad (2)$$

where R is the distance from the calculated point to the axis of the rotating tool. μ is the friction coefficient between the tool and the workpiece (supposed constant in this model). $w = 2\pi r$ is the angular velocity of the tool.

Two types of thermal boundary conditions are defined in this model. The heat flux boundary condition for the workpiece at the tool/workpiece interface is :

$$k \frac{\partial T}{\partial n} = q_{pin} \quad (3)$$

The convection boundary condition for all the workpiece surfaces exposed to the air can be expressed as :

$$k \frac{\partial T}{\partial n} = h(T - T_0) \quad (4)$$

n is the normal direction vector of boundary, and h is the convection coefficient and T_0 is the ambient temperature $(300K)$. The surface of the workpiece in contact with the backup plate is simplified to the convection condition with an effective convection.

4 Discussion and results

In the present study, experimental investigations of heat generation during FSP were performed. FSP experiments with different combinations of processing parameters were conducted and are listed in table 2. These experimental results were compared to numerical ones : the numerical temperature (maximal) was evaluated behind the tool by using the model introduced in the section before. A good correlation is observed between the experimental data and computational results . This shows that the proposed thermal model can be used to predict effect of the various FSP parameters on the temperature distribution. The simulated temperature history of FSP at different process parameter combinations are presented in Figure 2.

The temperature is the highest in the contact zone between the rotating tool and the workpiece. Behind the tool, the process transports hot material away, while in front of the tool, new cold material enters Figure 3.

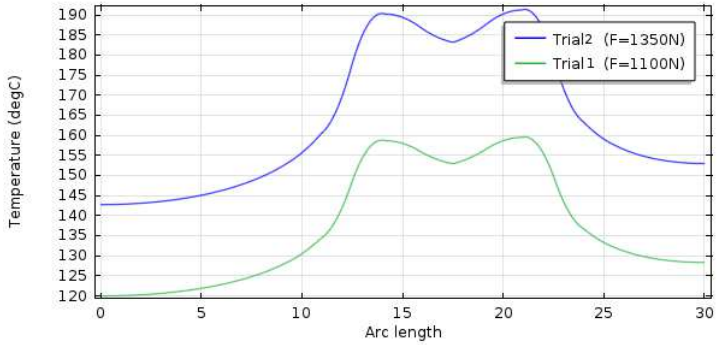

FIGURE 2 – Temperature history along the processing line

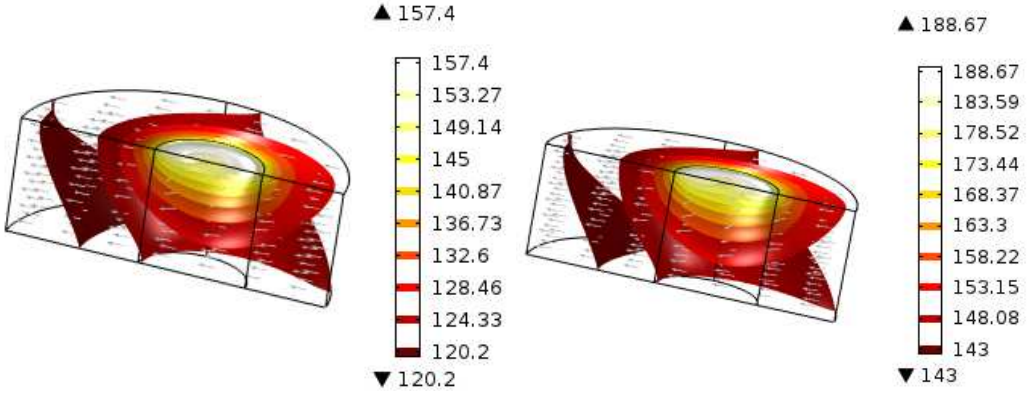

(a) Trial 1 (b) Trial 2

FIGURE 3 – Numerical temperature field

Infra-red camera data from FSP experiments along with predicted temperatures from two boundary conditions are shown in Table 2. In the experiment, the camera measurements show the maximum temperature experienced, which may occur slightly upstream or downstream of the pin. Generally, the experimental data and the two numerical results are in good agreement. The maximum predicted temperature for trial 1 and trial 2 are respectively 160^0C and 191 ^0C. The predicted temperatures at the retreating side are nearly identical to the measured values.

5 Conclusion

Our focus on this paper was to simulate the thermal behavior of the FSW tool during a complete friction stir process. The results of the thermal simulation have shown realistic performance. The main idea is to use this numerical model in an optimisation process of FSP. In a practical way, optimisation is synonymous with the use of long running and computationally intensive simulations. This type of model proposed in this paper is faster and simpler than thermomechanical one. So they are very efficient and convenient to run a first step of optimization. Then more complicated models can be used to refine the search.

Références

[1] S. Cartigueyen, O.P. Sukesh, and K. Mahadevan. Numerical and experimental investigations of heat generation during friction stir processing of copper. *Procedia Engineering*, 97 :1069 – 1078, 2014.

[2] M. Chiumenti, M. Cervera, C. Agelet de Saracibar, and N. Dialami. Numerical modeling of friction stir welding processes. *Computer Methods in Applied Mechanics and Engineering*, 254 :353–369, 2013.

[3] A.R. Darvazi and M. Iranmanesh. Thermal modeling of friction stir welding of stainless steel 304l. *The International Journal of Advanced Manufacturing Technology*, 75(9) :1299–1307, 2014.

[4] M. Folea, A.and Langlade C. Roman, E. Schlegel, D. ; Gete, and D. Chamoret. *Comprehensive Guide for Nanocoatings Technology, Volume 1 : Deposition and Mechanism*, chapter Producing Nanograin Surface Layers by Friction Stir Processing, pages 333–356. Nova Science Publishers : New York, 2015.

[5] N. D. Ghetiya, K. M. Patel, and Anup B. Patel. Prediction of temperature at weldline in air and immersed friction stir welding and its experimental validation. *The International Journal of Advanced Manufacturing Technology*, 79(5) :1239–1246, 2015.

[6] C. Langlade, A. Roman, D.Schlegel, E. Gete, P. Noel, and M. Folea. Friction stir process of b194 cooper-beryllium alloy. In *The 30th International Conference on Surface Modification Technologies*, Politecnico Di Milano, Campus Bovisa Milan, Italy, 29th June-1st July 2016.

[7] C. Langlade, A. Roman, D. Schlegel, E. Gete, and M. Folea. Formation of a tribologically transformed surface (tts) on aisi 1045 steel by friction stir processing. *Materials and Manufacturing Processes*, 31(12) :1565–1572, 2016.

[8] A. A. Larsen, M.P. Bendsøe, J. H. Hattel, and H. Schmidt. Optimization of friction stir welding using space mapping and manifold mapping : an initial study of thermal aspects. *Structural and Multidisciplinary Optimization*, 38(3) :289–299, 2009.

[9] Z.Y. Ma. Friction stir processing technology : A review. *Metallurgical and Materials Transactions A*, 39(3) :642–658, 2008.

[10] N. Rajamanickam and V. Balusamy. Numerical simulation of transient temperature in friction stir welding of aluminum alloy 2014 -t6. *Manufacturing engineering*, 2 :41–44, 2007.

[11] C. De Sansala, B. Devincre, and L. Kubin. Grain size strengthening in microcrystalline copper : A three-dimensional dislocation dynamics simulation. *, Mechanical properties of solids XI, Key Engineering Materials*, pages 25–32, 2010.

[12] M. Song and R. Kovacevic. Thermal modeling of friction stir welding in a moving coordinate system and its validation. *International Journal of Machine Tools and Manufacture*, 43(6) :605–615, 2003.